Nanoscale Advances

ROYAL SOCIETY OF CHEMISTRY

PAPER

View Article Online
View Journal | View Issue

Cite this: *Nanoscale Adv.*, 2025, **7**, 7527

Detection of microplastic release into water from plastic containers based on lensless digital holography

Liang Xue, Hao Chen, Hao Zhou, Yusheng Wu, Chunjuan Wei, Youhua Jiang and Hao Yang Cui*

Received 27th April 2025
Accepted 19th July 2025

DOI: 10.1039/d5na00407a

rsc.li/nanoscale-advances

This study effectively analyzed the impact of microplastic release. Plastic containers are widely used in the food delivery industry, but the released microplastic particles can pose a threat to human health and the environment. The study employs lensless digital holography, which utilizes the principles of near-field light scattering and optical interference to rapidly detect microplastic particles. By adjusting the reconstruction distance, the technique can differentiate microplastic particles from other impurities, achieving precise detection and analysis of microplastic particles. The results showed that the release of microplastic particles from plastic bags at room temperature was about 5.25 times that of plastic boxes. In the experiment of releasing microplastics from plastic boxes, the increase was 1158.82% after heating for 60 seconds, 132.48% after three heating cycles, 141.18% after refrigeration, and 21.37% after refrigeration before heating. This study reveals the release of microplastics under different treatment conditions, providing a reliable basis for reducing the harm of microplastics.

1. Introduction

With the rapid development of the food delivery industry and the increasing demand for convenient dining options, ordering takeout has become a common eating habit.[1] Studies have shown that the size of China's food delivery market has grown from 3.4 billion US dollars in 2011 to 32.5 billion US dollars in 2017.[2] Faced with such a massive demand for takeout, businesses have had to consider the storage and transportation of food, ultimately turning to convenient and inexpensive plastic containers.[3] However, the widespread use of plastic containers has inevitably led to microplastic pollution, posing threats to both the environment and human health.[4–6]

Microplastics are defined as plastic particles with diameters ranging from 1 micrometer to 5 millimeters,[7] varying in shape and size.[8] Based on their sources, microplastics can be classified into two categories: primary and secondary microplastics. Primary microplastics are directly produced as small plastic particles during industrial and product manufacturing processes, while secondary microplastics are tiny particles formed from the degradation of larger plastic waste in the natural environment due to physical, chemical, or biological processes.[9] Due to the small volume, wide distribution, and difficulty in being detected by the naked eye, microplastic particles are commonly found in daily life. This makes microplastics easily enter the human body, posing significant threats to the natural environment and human health.[10–13] Research has shown that microplastics can adversely affect human health through endocrine disruption, cumulative effects, and the transport of pathogens.[14,15]

Microplastics have a small volume that is difficult to observe with the naked eye, and their diverse shapes are easily confused with that of other particles. Currently, the mainstream detection method is spectroscopic analysis, which mainly includes Fourier transform infrared spectroscopy (FTIR) and Raman spectroscopy.[16,17] For instance, Feride Öykü Sefiloglu *et al.* used micro-FTIR to measure the mass concentration of microplastic particles in urban water samples,[18] while Viktória Parobková *et al.* employed Raman microspectroscopy to detect microplastic particles in human tonsils.[19] Although spectroscopic analysis is an effective method, its high cost of equipment and the need for professional operators make it inconvenient. Moreover, there needs to be a trade-off between sensitivity and speed.[20] In addition to spectroscopic analysis, some dye-based fluorescence microscopy methods can also effectively detect microplastic particles, such as Nile red, rhodamine B, and safranin. These methods can observe the distinct fluorescence emitted by microplastic particles under a fluorescence microscope. However, since their detection principle relies on the lipophilicity of the dyes, they cannot completely exclude interference from other non-microplastic organic particles. Moreover, the waste liquid from these chemical dyes can cause secondary environmental pollution.[21–24] Therefore, a low-cost and easy-to-operate method is urgently needed for microplastic detection.

College of Electronics and Information Engineering, Shanghai University of Electric Power, Shanghai, P. R. China. E-mail: cuihy@shiep.edu.cn

Currently, some studies have focused on the issue of microplastic particle release from plastic containers. For example, Can Xu *et al.* investigated the changes in microplastic particle release from polypropylene self-heating food containers during use and explored the impact of released volatile organic compounds on human health.[25] Xin Guo *et al.* studied the influence of oil on microplastic release from plastic packaging, filling the information gap regarding microplastics in edible oils.[26] Yet Yin Hee *et al.* examined the effects of storage conditions and washing on microplastic release from plastic containers and found that repeated washing increased the release of microplastic particles by an order of magnitude.[27] These studies provide a data foundation for understanding the mechanisms and patterns of microplastic release. However, they are mostly limited to single-factor considerations. In daily life, the usage scenarios of plastic containers are more complex, such as heating food in a microwave oven, refrigerating in a fridge, or even multiple cycles of heating and refrigeration. Under the dual influence of heating and refrigeration, the release of microplastics may also be subject to complex effects.[28–31] This makes it necessary to conduct in-depth research on the effects of different conditions on the release of microplastic particles from plastic containers, which helps to study the mechanism of microplastic release and provide more scientific usage recommendations for the public, reducing the potential risks of microplastics to human health.

In summary, an effective detection method for microplastic particles released from plastic containers under different processing conditions is necessary. Approaches that closely align with real-world application scenarios can better provide data support for assessing the risks of microplastic particle release. The lensless digital holography technology adopted in this study can effectively and conveniently detect microplastic particles released from plastic containers. It offers advantages such as simple operation, low cost, a large field of view, high precision, and compact size.[32,33] The CMOS camera used in this study has a pixel size of 3.45 μm × 3.45 μm and a resolution of 2448 × 2048. With a detection limit of 5 μm and an imaging field of view of approximately 24 mm^2, it ensures detection accuracy and the feasibility of rapid particle localization. Using a partially coherent light source LED enhances the coherence of light and eliminates speckle noise from lasers, thus providing a certain degree of anti-interference capability. In addition, the entire imaging process, including setting up the experimental apparatus, placing the glass slide, adding the sample to be tested, and capturing the hologram, takes approximately 5 minutes in total. The cost of the entire set of equipment is approximately 300 pounds, and it is suitable for detecting complex conditions that closely resemble real-life scenarios. Its principle involves using an LED light source to illuminate the sample through a slit, with a CMOS image sensor (Model: MV-CB050-11UC-C) recording the interference patterns of light waves. The captured images are then reconstructed using angular spectrum theory and phase retrieval techniques to ultimately obtain three-dimensional images.[34–36] Although lensless technology lacks the focusing and magnification functions of traditional microscopes and has limitations in resolution, post-image reconstruction processing can effectively compensate for this issue. Moreover, its large field of view is more conducive for observing the overall distribution of the sample. Based on these advantages, lensless digital holography technology holds promise for convenient and rapid detection of microplastic particles, providing data support for research on the threats posed by microplastic particles to dietary health in daily life.

2. Materials and methods

2.1. Material preparation

The plastic containers selected for the experiment are all made of polypropylene (PP). This is because the plastic materials commonly used for takeout containers typically include polypropylene (PP), polyethylene (PE), polystyrene (PS), and polyethylene terephthalate (PET). Among these, polyethylene, polystyrene, and polyethylene terephthalate have relatively poor heat resistance, making them unsuitable for daily microwave heating. Additionally, these materials tend to be rough and prone to aging and becoming brittle after repeated use. Overall, polypropylene takeout food containers are the most ideal experimental subjects for studying the release of microplastic particles. The polypropylene plastic containers and microplastic powders used in the experiment were purchased from a Chinese

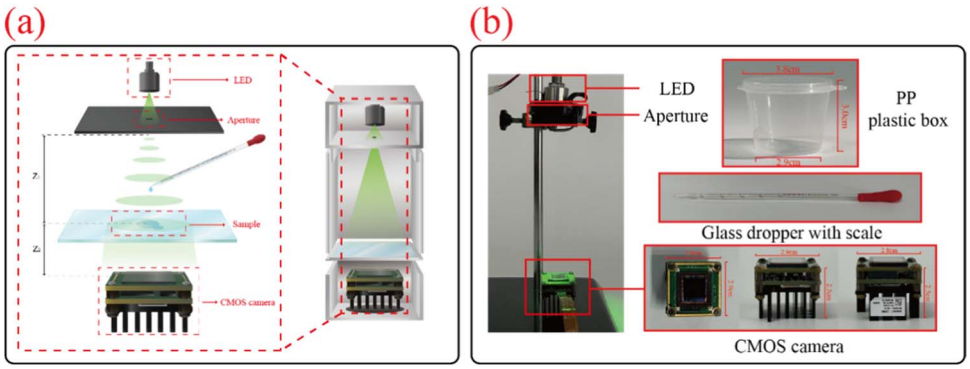

Fig. 1 Schematic diagram and set-up of the lensless holographic imaging experimental device; (a) schematic diagram of the lensless holographic imaging experimental device; (b) lensless holographic imaging experimental device and related material and equipment parameters.

online shopping platform (https://www.taobao.com/). To simulate the contact between takeout containers and food, distilled water was used as the medium to minimize interference from impurities in the water. The parameters of the experimental equipment and the physical image of the experiment are shown in Fig. 1(b). The experimental equipment parameters are as follows: the microwave power is 700 W and the refrigerator temperature is approximately 5–8 °C. The diameter of the various microplastic powders used in the experiment is about 5 μm. The number of microplastic particles in the experimental data is the average result of eight repeated experiments, and the microplastic abundance (MP/L) is calculated by proportionally converting the number of microplastic particles and the sample volume; the droppers used in the experiment were all glass droppers with scales. The plastic containers used in the experiment have a volume of 25 ml, with 15 ml of distilled water added for each experiment, and the contact area between the water and the plastic box container is approximately 26 cm^2.

2.2. Principle of lensless digital holography technology

Lensless digital holography technology is an advanced optical imaging technique based on wavefront information recording. Compared to traditional microscopes, this technology eliminates the need for complex and expensive lens systems. Instead, it uses a CMOS image sensor to directly record the interference patterns of light waves to capture sample information. The image captured by the CMOS camera is the hologram, which contains information about the phase, amplitude, and structure of the sample. The setup primarily consists of four components: a green LED light source with a central wavelength of 525 nm, an aperture, the sample under test, and a CMOS image sensor.

The principle of the experimental setup is illustrated in Fig. 1(a), where Z_1 represents the distance from the light source to the sample, and Z_2 represents the distance from the sample to the sensor. Since the distance from the sample to the CMOS image sensor is extremely small and much less than the distance from the LED light source to the sample, *i.e.*, $Z_1 \gg Z_2$, the short coherence length allows the use of a partially coherent LED light source. After passing through the aperture, the coherence of light is enhanced, effectively avoiding speckle noise generated by lasers and resulting in clearer interference images. At this point, the light is directed onto the sample being tested by partially coherent LED light sources. The scattered light from the sample and the transmitted light passing through the sample create a near-field interference effect, forming an interference pattern. Here, the scattered light $U_O(x,y)$ serves as the object wave, and the transmitted light $U_R(x,y)$ acts as the reference wave. The light waves propagate to the CMOS image sensor and are recorded, with the captured image being the hologram of the sample $H(x,y)$. The specific formula is as follows:

$$H(x,y) = U_O(x,y) + U_R(x,y) = A_R + A_O(x,y)\exp[i\phi_0(x,y)] \quad (1)$$

where A_O is the amplitude information of the object wave, A_R is the amplitude information of the reference wave, and ϕ_0 is the phase information of the object wave.

Since the transmitted light, as the reference wave, is relatively stable, while the scattered light has a more significant impact on the quality of the hologram, it is necessary to evaluate the effect of scattered light on the imaging quality of the hologram. The microplastic particles detected in this study have diameters ranging from 1 μm to 50 μm. The experiment uses a green LED light source with a wavelength of 525 nm, which meets the criterion for Mie scattering theory where the particle diameter is greater than or comparable to the incident light wavelength. Therefore, the scattering cross-section is used to evaluate the scattering ability of the particles, thereby assessing the imaging quality of the hologram. The distribution and phase information of the scattered light are calculated using Mie scattering theory. The specific formula is as follows:

$$C_s(\lambda) = \frac{2\pi}{k^2}\sum_{n=1}^{\infty}(2n+1)\left(|a_n|^2 + |b_n|^2\right) \quad (2)$$

where $C_s(\lambda)$ is the scattering cross-section, λ is the incident light wavelength (525 nm), k is the wavenumber, and a_n and b_n are the Mie scattering coefficients. The specific formulae are as follows:

$$a_n = \frac{m\psi_n(mx)\psi_n'(x) - \psi_n'(mx)\psi_n(x)}{m\xi_n(mx)\psi_n'(x) - \xi_n'(mx)\psi_n(x)} \quad (3)$$

$$b_n = \frac{\psi_n(mx)\psi_n'(x) - m\psi_n'(mx)\psi_n(x)}{\xi_n(mx)\psi_n'(x) - m\xi_n'(mx)\psi_n(x)} \quad (4)$$

where m is the ratio of the complex refractive index of the particle to that of the surrounding medium, x is the size parameter, and ψ_n and ξ_n are the first and third kinds of spherical Bessel functions, respectively.

2.3. Principle of holographic reconstruction

Lensless digital holography lacks the magnification and focusing capabilities of traditional lenses, resulting in low-resolution holograms captured by the CMOS sensor. To improve resolution, hologram reconstruction is necessary. This process uses optical interference and diffraction principles to recover the phase and amplitude information from the recorded interference patterns, thereby reconstructing a three-dimensional image. Common reconstruction algorithms include the Fresnel transform method, iterative methods, and the angular spectrum method. The Fresnel method can be numerically unstable and is limited by diffraction distance when dealing with high-resolution or large holograms. Iterative methods may fail to converge due to inappropriate initial phase distributions or constraints. In contrast, the angular spectrum method is stable, not limited by diffraction distance, and can more accurately recover the complex amplitude information of the object wave. Therefore, this study uses the angular spectrum method to reconstruct the hologram, simulating the optical diffraction process to recover the amplitude and phase information of the object wave. This allows for the reconstruction of

the external and internal features of microplastic particles. The reconstruction process is described by using the following formula:

$$U_c(x,y) = \mathcal{F}^{-1}\{\mathcal{F}[U_I(x,y)] \times H_{-Z_2}(x,y)\} \quad (5)$$

where $U_I(x,y)$ is the complex amplitude of the captured hologram, generally $U_I(x,y) = \sqrt{I(x,y)}$; $I(x,y)$ is the captured light intensity information; $U_c(x,y)$ is the complex amplitude of the reconstructed object; and $H_{-Z_2}(x,y)$ is the angular spectrum propagation, which propagates backward by a distance of Z_2. $H_{Z_2}(x,y)$ can be obtained by using the following formula:

$$H_{Z_2}(x,y) = \begin{cases} \exp\left(ikZ_2\sqrt{1-\lambda^2 f_x^{\,2}-\lambda^2 f_y^{\,2}}\right) & ,f_x^{\,2}+f_y^{\,2} < \dfrac{1}{\lambda^2} \\ 0 & ,f_x^{\,2}+f_y^{\,2} \geq \dfrac{1}{\lambda^2} \end{cases} \quad (6)$$

where λ is the wavelength of the LED light source (525 nm in this study); f_x and f_y are the spatial frequency coordinates; and Z_2 is the distance from the sample to the sensor.

2.4. Experimental design for simulating microplastic release

In the everyday use of plastic containers, people often store food in the refrigerator or freezer, or reheat food in the microwave. There may even be cases of multiple cycles of heating and refrigeration. During this process, the release of microplastic particles may vary with factors such as heating time, heating frequency, refrigeration time, and container material. Therefore, it is necessary to summarize the relationship between different treatment methods and changes in microplastic particle release. Additionally, some studies have suggested that the release of microplastic particles decreases when plastic containers are stored at low temperatures. Therefore, a comparison was made between heating plastic containers after refrigerated storage and storing them at room temperature and heating them to explore the inhibitory effect of refrigeration on the release of microplastic particles.

Fig. 2 shows the flowchart of image acquisition and reconstruction for detecting microplastic particles using lens-free holography. It includes the entire process from sample preparation to image acquisition and reconstruction, ultimately obtaining the reconstructed image and phase image of the microplastic particles.

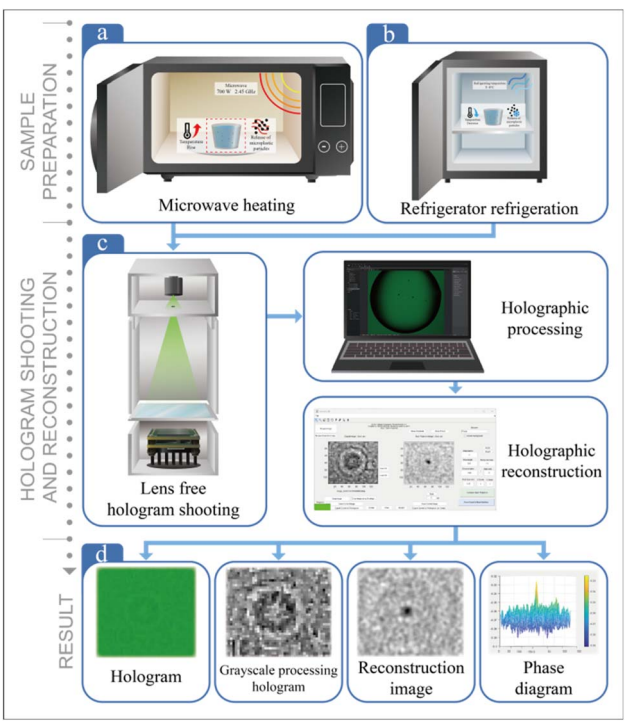

Fig. 2 Flow chart of image acquisition and reconstruction for detecting microplastic particles using lensless holographic technology; (a) and (b) preparation of experimental microplastic samples, including microwave heating and refrigeration in a refrigerator, (c) lens free image capture and reconstruction, (d) image reconstruction results, including holographic images of microplastic particles, grayscale processed holographic images of microplastic particles, reconstructed images of microplastic particles, and phase maps of microplastic particles.

3. Results

To ensure the reliability and generalizability of the experimental results and to reduce the impact of random factors, the results of the comparative experiments are the average values of eight repeated experiments.

3.1. Impact of different types of plastic containers

When investigating the impact of different types of plastic containers on the release of microplastic particles, we found that after storing a plastic box at room temperature for 30 days, the microplastic abundance was approximately 167 500 MP/L, while after refrigeration for 30 days, it is approximately 242 500 MP/L. The microplastic abundance increased by 44.81% after refrigeration compared to room temperature storage. The microplastic abundance after storing the plastic bag at room temperature for 30 days is approximately 880 000 MP/L, while after refrigeration for 30 days, it is approximately 192 500 MP/L. The microplastic abundance increased by 357.14% after room

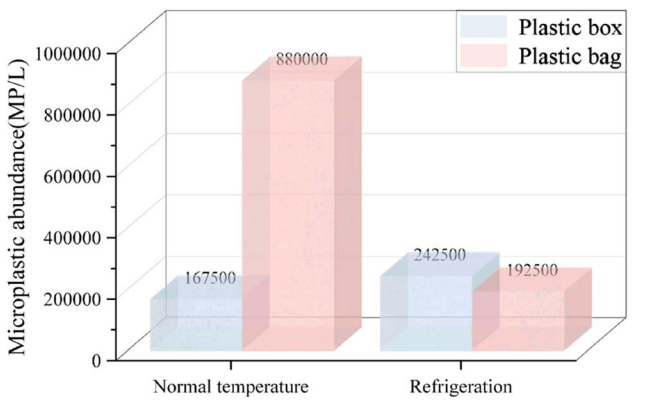

Fig. 3 Comparison of microplastic abundance in plastic boxes and plastic bags stored at room temperature and in a refrigerator.

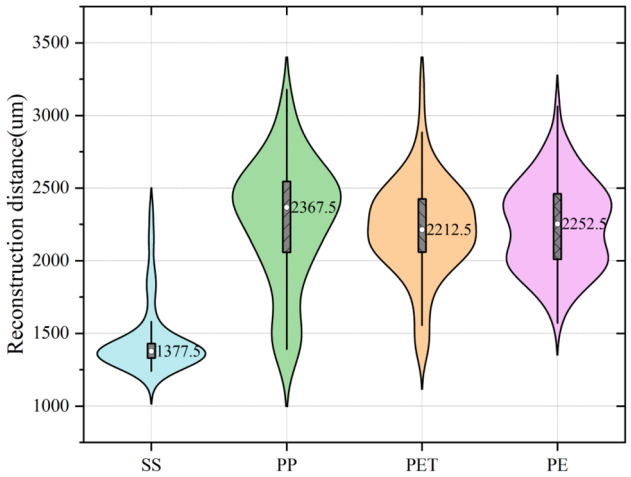

Fig. 4 Reconstruction distance distribution of suspended particles in water and microplastic particles of different materials.

temperature storage compared to refrigeration. The release of microplastic particles from plastic bags at room temperature is about 5.25 times that of plastic boxes. Considering that plastic bags cannot be heated in a microwave oven, the experimental subjects in this study all used polypropylene plastic boxes. Fig. 3 shows the comparison of the abundance of microplastic particles released from polypropylene plastic boxes and plastic bags after a period of storage under room temperature and refrigerated conditions.

3.2. Analysis of the microplastic reconstruction distance

Based on the imaging principle of lensless digital holography, the closer a particle is to the photosensitive area of the CMOS image sensor, the smaller its reconstruction distance will be during hologram reconstruction. Since different types of microplastics have different densities, and their positions in water after settling for a period of time will vary, leading to different optimal reconstruction distances. Therefore, the type of microplastic can be determined by its optimal reconstruction distance. The plastic containers used in this study are made of polypropylene due to its heat resistance and stability. However, during the experiment, external environmental factors and experimental operations may introduce additional contamination, such as air pollution, leading to the presence of microplastic particles of other materials and impurities in the sample. Therefore, this study detected the three most common microplastic materials in air (PP, PET, and PE) as well as impurity particles in the hologram. During the experiment, each sample was allowed to settle for 90 seconds before capturing the image to ensure that the microplastic particles fully settled in the water. The detection time was also strictly

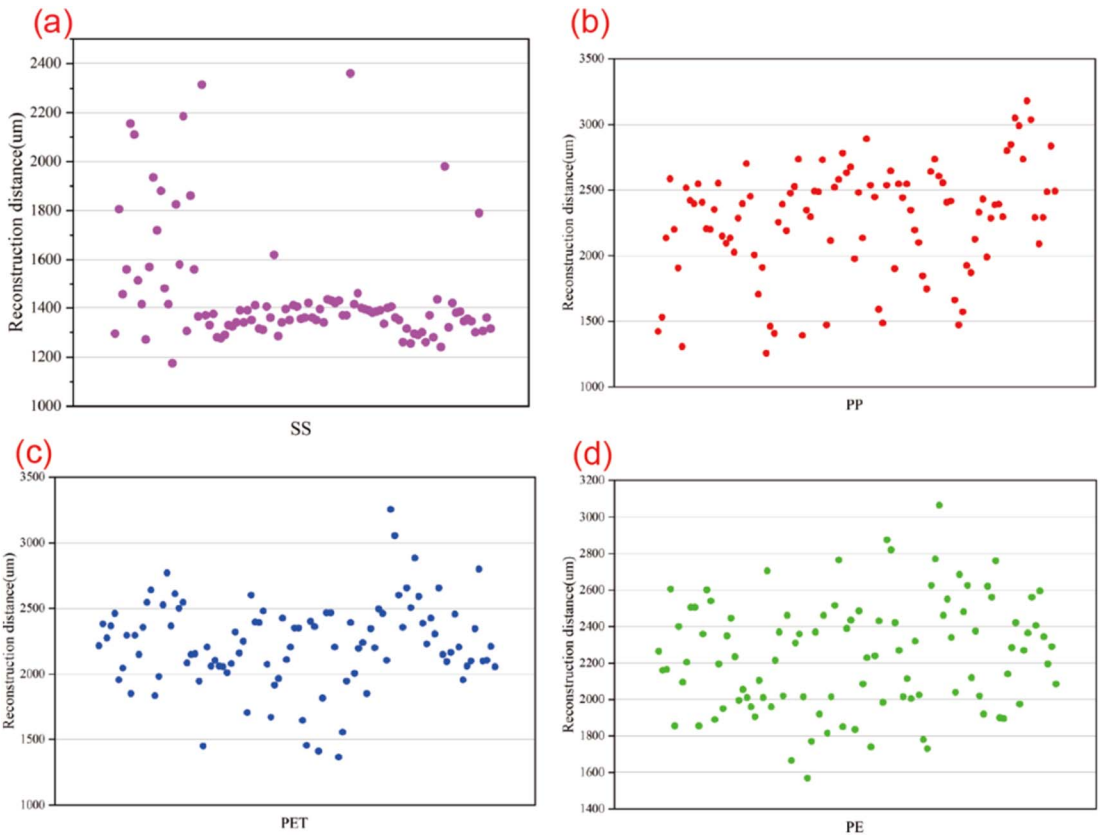

Fig. 5 Scatter plot of reconstruction distances for suspended particles in water and microplastic particles; (a) reconstruction distance of suspended particles in water; (b) reconstruction distance of PP microplastics; (c) reconstruction distance of PET microplastics; (d) reconstruction distance of PE microplastics.

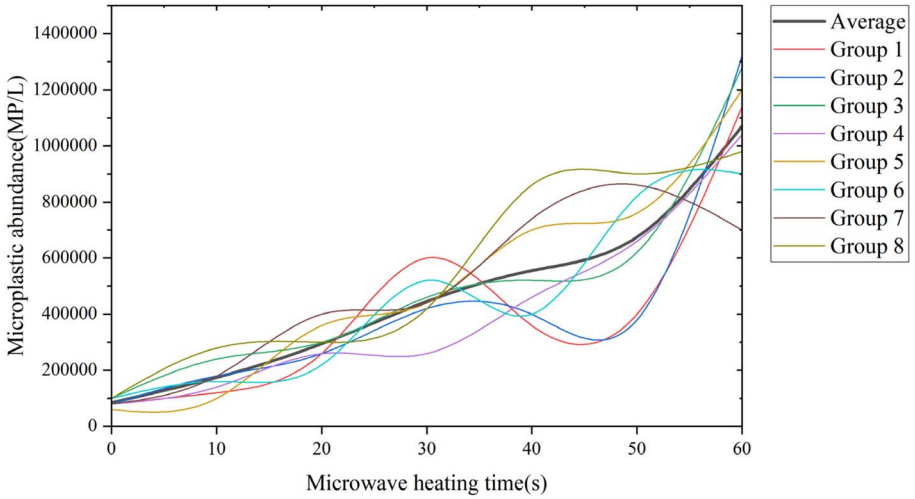

Fig. 6 Impact of microwave heating time on microplastic release.

controlled to avoid the coffee ring effect caused by prolonged exposure to a light source, which could lead to inaccurate results.

To obtain the optimal reconstruction distance range for microplastic particles of different materials, this study artificially added microplastic powders to the test samples for detection. Both the microplastic particles and the suspended solid (SS) particles captured in water were reconstructed, with 100 particles of each material being reconstructed. The diameter of these particles is about 5 μm. Among them, the reconstruction distance of the SS particles is concentrated in the range of 1200 to 1600, with a median of 1377.5. The density of PP is 0.91 g cm^{-3}, and it floats on the water surface. The reconstruction distance is concentrated between 2050 and 2550, with a median of 2367.5. The density of PET is 1.38 g cm^{-3}, and it settles in the water. The reconstruction distance is concentrated between 2050 and 2400, with a median of 2212.5. The density of PE is 0.95 g cm^{-3}, and it floats on the water surface. The reconstruction distance is concentrated between 2000 and 2450, with a median of 2252.5. Fig. 4 shows the reconstruction distance distribution of SS particles and the three types of microplastic particles. Fig. 5 shows the scatter plot of the reconstruction distances for 100 particles each of the SS particles and the three types of microplastics.

3.3. Impact of microwave heating time

When investigating the impact of microwave heating duration on the release of microplastic particles, we found that without heating, the abundance of microplastics was approximately 85 000 MP/L. After 10 seconds of microwave heating, the microplastic abundance increases to approximately 175 000 MP/L. After 20 seconds, it reaches approximately 295 000 MP/L. After 30 seconds, it is approximately 445 000 MP/L. After 40 seconds, it is approximately 555 000 MP/L. After 50 seconds, it is approximately 675 000 MP/L. After 60 seconds, it reaches approximately 1 070 000 MP/L. The growth rate from no heating to 10 seconds of heating is 105.88%, from 10 to 20 seconds is 68.57%, from 20 to 30 seconds is 50.85%, from 30 to 40 seconds is 24.72%, from 40 to 50 seconds is 21.62%, and from 50 to 60 seconds is 58.52%. The growth rate without heating for 60 seconds is 1158.82%. The specific data are shown in Fig. 6, which includes the results of eight independent replicate experiments and their arithmetic means.

3.4. Impact of single heating and multiple heating

When investigating the impact of the number of microwave heating cycles on the release of microplastic particles, we found that a single 60 second microwave heating session resulted in a microplastic abundance of approximately 1 070 000 MP/L. After two 30 second heating sessions, it is approximately 1 690 000 MP/L. After three 20 second heating sessions, it is approximately 2 487 500 MP/L. When the total heating time is the same, it can be observed that compared to single microwave heating, the microplastic abundance increases by 58% for two heating cycles and by 132.48% for three heating cycles. The specific data are shown in Fig. 7.

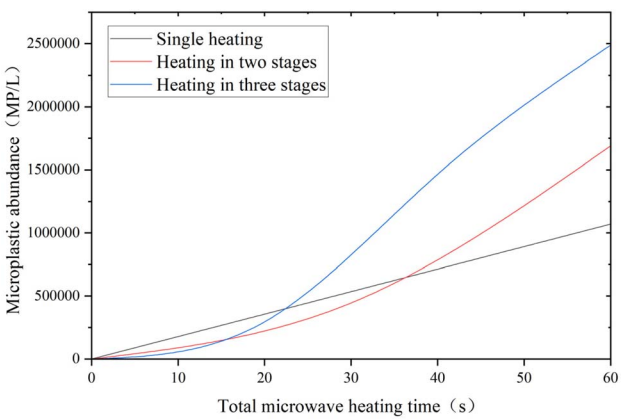

Fig. 7 Impact of microwave heating frequency on microplastic release.

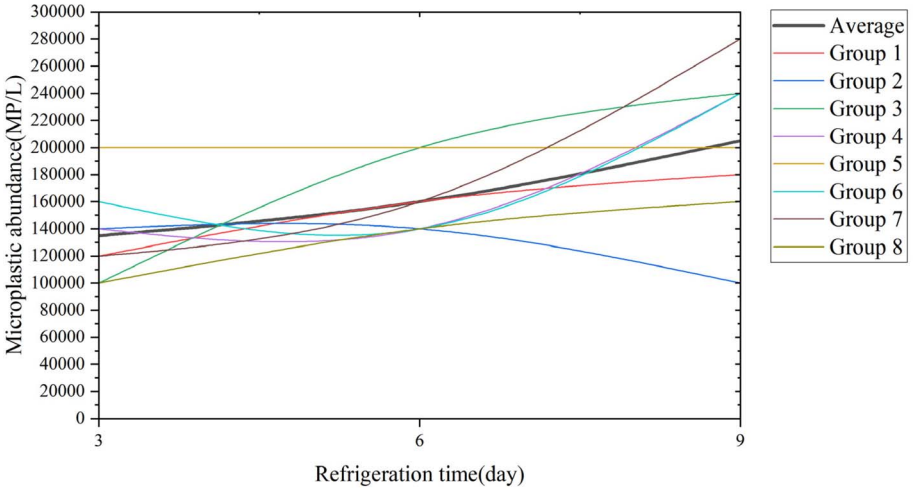

Fig. 8 Impact of refrigeration time on microplastic release.

3.5. Impact of refrigeration time

When investigating the impact of refrigeration duration on the release of microplastic particles, we found that at room temperature, the abundance of microplastics was approximately 85 000 MP/L. After 3 days of refrigeration, the microplastic abundance is approximately 135 000 MP/L. After 6 days, it is approximately 160 000 MP/L. After 9 days, it is approximately 205 000 MP/L. The growth rate from 3 to 6 days is 18.52%, and from 6 to 9 days is 28.13%. The growth rate of microplastic abundance from room temperature to 9 days of refrigeration is 141.18%. Fig. 8 illustrates the effect of refrigeration duration on the release of microplastic particles, with data including the results of eight independent replicate experiments and their arithmetic means.

3.6. Impact of refrigeration before heating

When investigating the impact of whether the sample was refrigerated before heating on the release of microplastic particles, we found that the microplastic abundance was approximately 445 000 MP/L after direct heating for 30 seconds. After refrigeration for 3 days followed by heating, it is approximately 442 500 MP/L, a decrease of 0.56%. After the second 30 second heating session without refrigeration, the microplastic abundance is approximately 1 690 000 MP/L. After refrigeration for 3 days followed by heating, it is approximately 1 567 500 MP/L, a decrease of 7.25%. After the third 30 second heating session without refrigeration, the microplastic abundance is approximately 2 362 500 MP/L. After refrigeration for 3 days followed by heating, it is approximately 1 857 500 MP/L, a decrease of 21.37%. Fig. 9 shows the effect of whether refrigeration was conducted before heating on the release of microplastic particles, with data including the results of eight independent replicate experiments and their arithmetic means.

3.7. Microplastic reconstruction analysis

Fig. 10 shows the reconstruction and phase images of impurity particles and microplastic particles and contain relevant information about the target particles during the reconstruction process. The reconstructed images can help us identify the types of particles and exclude the interference from impurity

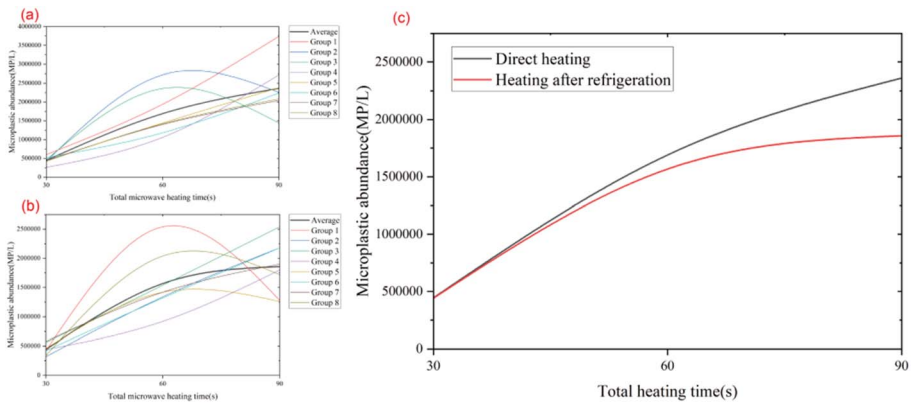

Fig. 9 (a) Changes in microplastic abundance and average curve for eight experiments with direct microwave heating. (b) Changes in microplastic abundance and average curve for eight experiments with refrigeration before microwave heating. (c) Comparison of average microplastic abundance curves for direct heating and refrigeration before heating.

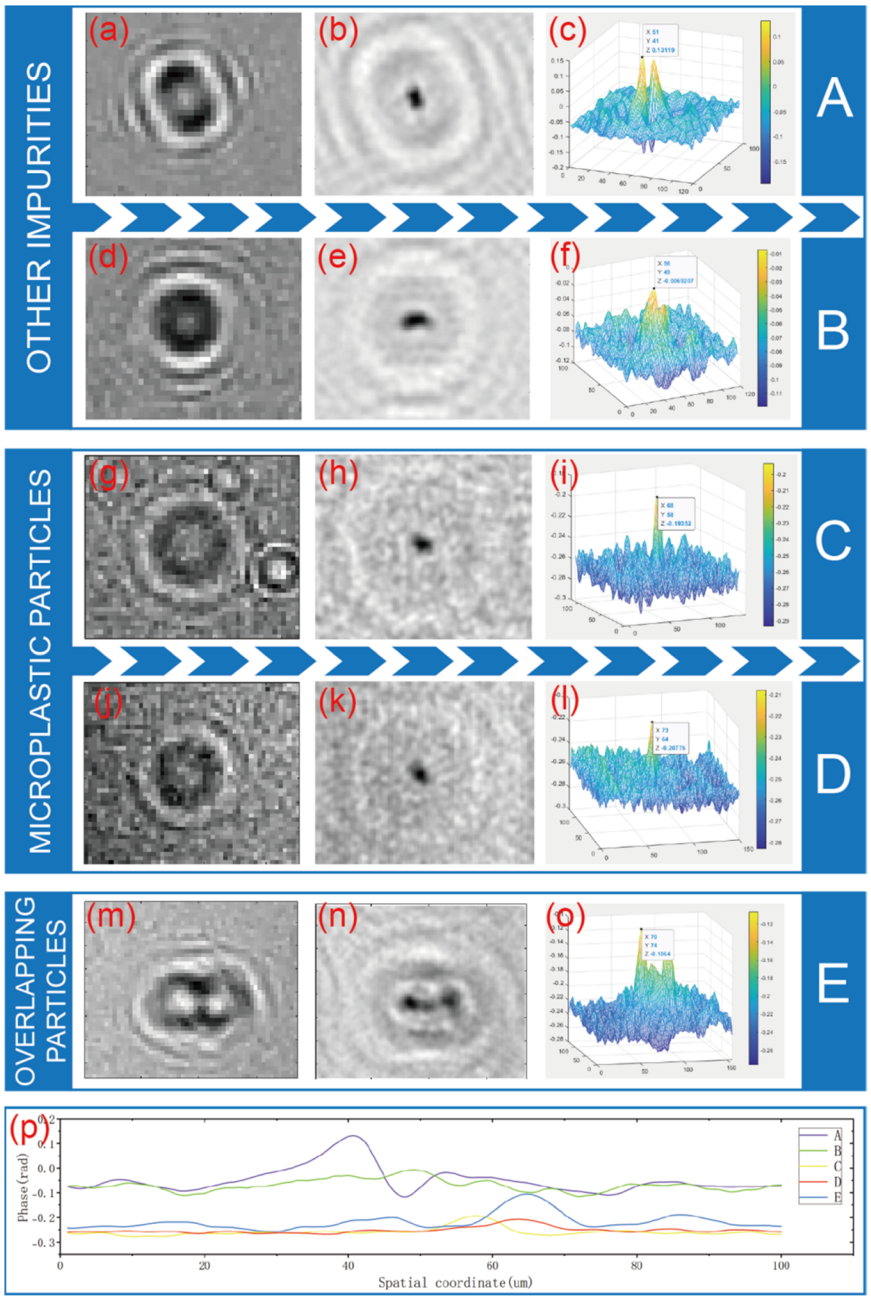

Fig. 10 Reconstruction and phase diagram of impurity particles and microplastic particles; (a), (b), and (c) and (d), (e), and (f) are the holograms, reconstructed images, and phase maps of impurity particles A and B, respectively; (g), (h), and (i) and (j), (k), and (l) are the holograms, reconstructed images, and phase maps of microplastic particles C and D, respectively; (m), (n), and (o) are holograms, reconstructed images, and phase maps of partially overlapping microplastic particles E; (p) comparison curves of cross-sectional strength for particles A, B, C, D, and E.

particles and overlapping microplastic particles. By analyzing the cross-sectional intensity distribution of the particles, the morphological features of the target particles can be further analyzed, aiding in the differentiation of microplastic particles from other impurities.

4. Discussion

Lensless digital holography has many advantages in detecting microplastic particles, such as small size, simple operation, low cost, guaranteed resolution and image quality, and large field-of-view imaging that is conducive to rapid positioning, providing a reliable means for research on microplastics.

In this study, plastic boxes made of polypropylene material were used, and glass was employed to isolate the samples to be tested to prevent air pollution. It was found that plastic boxes release more microplastic particles when stored in the refrigerator than at room temperature, which may be due to the contraction of the container at low temperatures, causing

Table 1 Summary of experimental types, conditions, and results

Experimental type	Experimental condition	Experimental result
Plastic box storage	Storage at room temperature	167 500 MP/L
	Storage in a refrigerator	242 500 MP/L
Plastic bag storage	Storage at room temperature	880 000 MP/L
	Stored in a refrigerator	192 500 MP/L
The influence of microwave heating time	Unheated	85 000 MP/L
	Heat for 10 seconds	175 000 MP/L
	Heat for 20 seconds	295 000 MP/L
	Heat for 30 seconds	445 000 MP/L
	Heat for 40 seconds	555 000 MP/L
	Heat for 50 seconds	675 000 MP/L
	Heat for 60 seconds	1 070 000 MP/L
The influence of microwave heating frequency	Single heating	1 070 000 MP/L
	Heating in two stages	1 690 000 MP/L
	Heating in three stages	2 487 500 MP/L
The influence of refrigerator storage time	Refrigerate for three days	135 000 MP/L
	Refrigerate for six days	160 000 MP/L
	Refrigerate for nine days	205 000 MP/L
The influence of whether refrigeration was conducted before heating	Heat directly for 30 seconds	445 000 MP/L
	Refrigerate for three days before heating for 30 seconds	442 500 MP/L
	Heat for 30 seconds for the second time	1 690 000 MP/L
	Refrigerate for three days again, then heat for 30 seconds for the second time	1 567 500 MP/L
	Heat for 30 seconds for the third time	2 362 500 MP/L
	Refrigerate for three days again, then heat for 30 seconds for the third time	1 857 500 MP/L

damage to the plastic structure. Plastic bags release far more microplastic particles at room temperature storage than at refrigerated storage, and release more microplastic particles than plastic boxes at room temperature storage, while the difference between the two is not significant at refrigerated storage. This is because plastic bags are more susceptible to external stress and have an uncontrollable contact area with water.

In the microwave heating experiment, as the heating time increased, the abundance of microplastics first increased sharply and then tended to stabilize, before increasing significantly again at the end, corresponding to the process of plastic structure damage, temperature stabilization, and exceeding the threshold. Under the same heating time, multiple heating cycles release more microplastic particles than a single heating cycle due to the accumulation of thermal damage.

In the refrigerator storage experiment, as the storage time increased, the abundance of microplastics slowly increased, which may be due to plastic cracking caused by low temperatures. After refrigeration and then heating, fewer microplastic particles are released compared to direct heating, as particles tend to aggregate at low temperatures. The specific experimental data are summarized in Table 1.

Compared with other studies, this research focuses more on the impact of everyday equipment on the release of microplastic particles, reminding people to pay attention to the microplastic risks in daily life and contributing to the prevention of microplastic pollution.

5. Conclusion

This study proposes a method for detecting microplastic particles based on lensless digital holography technology, with a focus on studying the effects of different processing conditions on the release of microplastic particles. This method utilizes the principles of near-field light scattering and light interference to achieve rapid detection of microplastic particles in water. Compared to traditional microscopes, it offers advantages such as compact size, simple operation, low cost, and low environmental requirements. Due to the varying densities of different particles, it is possible to distinguish between microplastic particles and other impurity particles by comparing the reconstructed distances. The study investigates the patterns of microplastic particle release from plastic containers by comparing variables such as microwave heating time, the number of microwave heating cycles, refrigerator storage time, whether the containers were refrigerated before microwave heating, and the differences between plastic boxes and plastic bags. The final results show that as the microwave heating time, the number of microwave heating cycles, and the refrigerator storage time increase, the abundance of microplastics increases significantly. In the case of heating after refrigeration, the abundance of microplastics is slightly lower compared to heating at room temperature. Lensless digital holography technology has significant potential for detecting particles, enabling rapid detection of microplastic particles. This not only helps to reveal the reasons for the release of microplastic particles influenced by the environment and raises

awareness of related issues but also helps to prevent the further spread of microplastic pollution, making a significant contribution to the suppression of microplastic pollution and the protection of human health.

Data availability

All data needed to evaluate the conclusions in the paper are present in the paper and/or the ESI.

Author contributions

Conceptualization: L. X., H. C. and H. Z.; methodology: L. X., H. C. and H. Z.; investigation: H. C., H. Z. and Y. S. W.; visualization: L. X., H. C., C. J. W. and Y. H. J.; supervision: L. X., H. Z., C. J. W., Y. H. J. and H. Y. C.; writing – original draft: H. C. and H. Z.; writing – review & editing: L. X., H. C., H. Z., and Y. S. W.

Conflicts of interest

The authors declare that they have no competing interests.

Acknowledgements

This work was supported by the National Natural Science Foundation of China (62105196). This research was supported by grants from the Engineering Research Center of Offshore Wind Technology Ministry of Education (Shanghai University of Electric Power).

References

1 Y. Choi, L. Zhang, J. Debbarma and H. Lee, Sustainable Management of Online to Offline Delivery Apps for Consumers' Reuse Intention: Focused on the Meituan Apps, *Sustainability*, 2021, **13**(7), 3593, DOI: **10.3390/su13073593**.

2 X. Zhao, W. Lin, S. Cen, H. Zhu, M. Duan, W. Li and S. Zhu, The online-to-offline (O_2O) food delivery industry and its recent development in China, *Eur. J. Clin. Nutr.*, 2021, **75**(2), 232–237, DOI: **10.1038/s41430-020-00842-w**.

3 A. Balik and V. J. E. Saija, Tanggungjawab Pemerintah Dan Pelaku Usaha Makanan Siap Saji Terkait Penggunaan Wadah Plastik Yang Berbahaya Bagi Konsumen Di Kota Ambon, *SASI*, 2018, **23**(2), 95–107, DOI: **10.47268/sasi.v23i2.103**.

4 Z. Ma, Y. Ibrahim and Y. Lee, Microplastic Pollution and Health and Relevance to the Malaysia's Roadmap to Zero Single-Use Plastics 2018–2030, *Malays. J. Med. Sci.*, 2020, **27**(3), 1–6, DOI: **10.21315/mjms2020.27.3.1**.

5 Z. H. Kong, F. J. Burdon, T. Amélie, M. Bundschuh, M. N. Futter, R. Hurley and B. G. McKie, Comparing effects of microplastic exposure, FPOM resource quality, and consumer density on the response of a freshwater particle feeder and associated ecosystem processes, *Aquat. Sci.*, 2023, **85**(3), 70, DOI: **10.1007/s00027-023-00964-w**.

6 T. Jin, Y. Liu, H. Lyu, Y. He, H. Sun, J. Tang and B. Xing, Plastic takeaway food containers may cause human intestinal damage in routine life usage: microplastics formation and cytotoxic effect, *J. Hazard. Mater.*, 2024, **475**, 134866, DOI: **10.1016/j.jhazmat.2024.134866**.

7 C. M. Rochman, A. L. Andrady, S. Dudas and J. Fabres, Sources, fate and effects of microplastics in the marine environment: Part 2 of a global assessment, *IMO/FAO/Unesco-IOC/WMO/IAEA/UN/UNEP Joint Group of Experts on the Scientific Aspects of Marine Environmental Protection (GESAMP)*, 2015, p. 93, DOI: **10.1016/j.marpolbul.2015.02.008**.

8 K. Mabadahanye, M. T. B. Dalu and T. Dalu, Occurrence and Removal of Microplastics in Wastewater Treatment Plants: Perspectives on Shape, Type, and Density, *Water*, 2024, **16**(12), 1750, DOI: **10.3390/w16121750**.

9 J. A. Conesa and N. Ortuño, Reuse of water contaminated by microplastics, the effectiveness of filtration processes: A review, *Energies*, 2022, **15**(7), 2432, DOI: **10.3390/en15072432**.

10 C. M. R. Almeida, I. Sáez-Zamacona, D. M. Silva, S. M. Rodrigues, R. Pereira and S. Ramos, The Role of Estuarine Wetlands (Saltmarshes) in Sediment Microplastics Retention, *Water*, 2023, **15**(7), 1382, DOI: **10.3390/w15071382**.

11 K. Bexeitova, A. Baimenov, E. A. Varol, K. Kudaibergenov, U. Zhantikeyev, Y. Sailaukhanuly, K. Toshtay, Z. Tauanov, S. Azat and R. Berndtsson, Microplastics in freshwater systems: A review of classification, sources, and environmental impacts, *Chem. Eng. J. Adv.*, 2024, 100649, DOI: **10.1016/j.ceja.2024.100649**.

12 J. Zhou, X. Liu, W. Li and Y. Cao, Characteristics, sources, and distribution of microplastics in sediments and their potential ecological risks: A case study in a typical urban river of China, *J. Environ. Chem. Eng.*, 2024, **12**(6), DOI: **10.1016/j.jece.2024.114575**.

13 E. B. Jadhav, M. S. Sankhla, R. Bhat and D. S. Bhagat, Microplastics from food packaging: An overview of human consumption, health threats, and alternative solutions, *Environ. Nanotechnol., Monit. Manage.*, 2021, **16**, 100608, DOI: **10.1016/j.enmm.2021.100608**.

14 O. S. Chowdhury, P. J. Schmidt, W. B. Anderson and M. B. Emelko, Advancing evaluation of microplastics thresholds to inform water treatment needs and risks, *Environ. Health*, 2024, **2**(7), 441–452, DOI: **10.3390/eh2040700**.

15 J. C. Prata, J. P. D. Costa, I. Lopes, A. L. Andrady, A. C. Duarte and T. R. Santos, A One Health perspective of the impacts of microplastics on animal, human and environmental health, *Sci. Total Environ.*, 2021, **777**, 146094, DOI: **10.1016/j.scitotenv.2021.146094**.

16 I. Chakraborty, S. Banik, R. Biswas, T. Yamamoto, H. Noothalapati and N. Mazumder, Raman spectroscopy for microplastic detection in water sources: a systematic review, *Int. J. Environ. Sci. Technol.*, 2023, **20**(9), 10435–10448, DOI: **10.1007/s13762-022-04505-0**.

17 K. Hu, D. Li, X. Cui, D. Hu, J. Chen, S. Zhuan, H. Chang, Y. Zhang, T. An and J. Zhang, Evaluation Of Monitoring

Technologies And Methods For Micro Plastics In Water As Novel Pollutants: The Exploration Of Accurate Quantitative Analysis And Efficient Screening, *Scalable Computing: Practice and Experience*, 2024, **25**(2), 729–738, DOI: 10.12694/scpe.v25i2.2548.

18 F. Sefiloglu, C. N. Stratmann, M. Brits, M. J. M. Velzen, Q. Groenewoud, A. D. Vethaak, R. Dris, J. Gasperi and M. H. Lamoree, Comparative microplastic analysis in urban waters using μ-FTIR and Py-GC-MS: A case study in Amsterdam, *Environ. Pollut.*, 2024, **351**, DOI: 10.1016/j.envpol.2024.124088.

19 V. Parobková, D. Holub, M. Kizovský, G. Kalčíková, U. Rozman, M. Urík, K. Novotný, O. Samek, T. Zikmund, P. Pořízka and J. Kaiser, Raman microspectroscopy and laser-induced breakdown spectroscopy for the analysis of polyethylene microplastics in human soft tissues, *Heliyon*, 2024, **10**(18), e18753, DOI: 10.1016/j.heliyon.2024.e18753.

20 C. Wang and P. Sahay, Breath Analysis Using Laser Spectroscopic Techniques: Breath Biomarkers, Spectral Fingerprints, and Detection Limits, *Sensors*, 2009, **9**(10), 8230–8262, DOI: 10.3390/s91008230.

21 H. A. Nel, A. J. Chetwynd, L. Kelleher, I. Lynch, I. Mansfield, H. Margenat, S. Onoja, P. G. Oppenheimer, G. H. S. Smith and S. Krause, Detection limits are central to improve reporting standards when using Nile Red for microplastic quantification, *Chemosphere*, 2020, **263**, 127953, DOI: 10.1016/j.chemosphere.2020.127953.

22 C. Wang, L. Jiang, R. Liu, M. He, X. Cui and C. Wang, Comprehensive assessment of factors influencing Nile red staining: Eliciting solutions for efficient microplastics analysis, *Mar. Pollut. Bull.*, **171**, 112698, DOI: 10.1016/j.marpolbul.2021.112698.

23 J. C. Prata, I. F. Sequeira, S. S. Monteiro, A. L. P. Silva, J. P. Costa, P. D. Pereira, A. J. S. Fernandes, F. M. Costa, A. C. Duarte and T. R. Santos, Preparation of biological samples for microplastic identification by Nile Red, *Sci. Total Environ.*, 2021, **783**, 147065, DOI: 10.1016/j.scitotenv.2021.147065.

24 L. Nalbone, A. Panebianco, F. Giarratana and M. Russell, Nile Red staining for detecting microplastics in biota: Preliminary evidence, *Mar. Pollut. Bull.*, 2021, **172**, 112888, DOI: 10.1016/j.marpolbul.2021.112888.

25 C. Xu, J. L. Hu, B. Dong, Q. Lin, S. Wu, J. Chen, J. Wang, D. Li and H. Zhong, Safety assessment of polypropylene self-heating food container: The release of microplastics and volatile organic compounds, *Food Packag. Shelf Life*, 2024, **44**, DOI: 10.1016/j.fpsl.2024.101307.

26 X. Guo, H. Dai, J. Gukowsky, X. Tan and L. He, Detection and quantification of microplastics in commercially bottled edible oil, *Food Packag. Shelf Life*, 2023, **38**, DOI: 10.1016/j.fpsl.2023.101122.

27 Y. Y. Hee, K. Weston and S. Suratman, The effect of storage conditions and washing on microplastic release from food and drink containers, *Food Packag. Shelf Life*, 2022, **32**, DOI: 10.1016/j.fpsl.2022.100826.

28 Y. J. He, Y. Qin, T. L. Zhang, Y. Y. Zhu, Z. J. Wang, Z. S. Zhou, T. Z. Xie and X. D. Luo, Migration of (non-) intentionally added substances and microplastics from microwavable plastic food containers, *J. Hazard. Mater.*, 2021, **417**, 126074, DOI: 10.1016/j.jhazmat.2021.126074.

29 E. Moreno-Gordaliza, M. D. Marazuela and M. M. Gomez-Gomez, Risk assessment of silver and microplastics release from antibacterial food containers under conventional use and microwave heating, *Food Chem.*, 2023, **420**, 136097, DOI: 10.1016/j.foodchem.2023.136097.

30 K. A. Hussain, S. Romanova, I. Okur, D. Zhang, J. Kuebler, X. Huang, B. Wang, L. Fernandez-Ballester, Y. Lu, M. Schubert and Y. Li, Assessing the Release of Microplastics and Nanoplastics from Plastic Containers and Reusable Food Pouches: Implications for Human Health, *Environ. Sci. Technol.*, 2023, **57**(26), 9782–9792, DOI: 10.1021/acs.est.3c01942.

31 V. C. Shruti and G. Kutralam-Muniasamy, Migration testing of microplastics in plastic food-contact materials: Release, characterization, pollution level, and influencing factors, *Trends Anal. Chem.*, 2024, **170**, DOI: 10.1016/j.trac.2023.117421.

32 J. Chen, W. Han, L. Fu, Z. Lv, H. Chen, W. Fang, J. Hou, H. Yu, X. Huang and L. Sun, A Miniaturized and Intelligent Lensless Holographic Imaging System With Auto-Focusing and Deep Learning-Based Object Detection for Label-Free Cell Classification, *IEEE Photonics J.*, 2024, **16**, 3900208, DOI: 10.1109/JPHOT.2024.3385182.

33 X. Hu, R. Abbasi and S. Wachsmann-Hogiu, Microfluidics on lensless, semiconductor optical image sensors: challenges and opportunities for democratization of biosensing at the micro-and nano-scale, *Nanophotonics*, 2023, **12**(21), 3977–4008, DOI: 10.1515/nanoph-2023-0301.

34 J. Picazo-Bueno, K. Trindade, M. Sanz and V. Micó, Design, Calibration, and Application of a Robust, Cost-Effective, and High-Resolution Lensless Holographic Microscope, *Sensors*, 2022, **22**, 553, DOI: 10.3390/s22020553.

35 A. Molani, F. Pennati, S. Ravazzani, A. Scarpellini, F. M. Storti, G. Vegetali, C. Paganelli and A. Aliverti, Advances in Portable Optical Microscopy Using Cloud Technologies and Artificial Intelligence for Medical Applications, *Sensors*, 2024, **24**, 6682, DOI: 10.3390/s24206682.

36 T. Wu, Y. Yang, H. Wang, H. Chen, H. Zhu, J. Yu and X. Wang, Investigation of an Improved Angular Spectrum Method Based on Holography, *Photonics*, 2024, **11**(1), 16, DOI: 10.3390/photonics11010016.